Impact of Electrolyte Anions on the Adsorption of CO on Cu Electrodes

Vincent J. Ovalle and Matthias M. Waegele*

Department of Chemistry, Merkert Chemistry Center, Boston College, Chestnut Hill, Massachusetts 02467, United States

E-mail: waegele@bc.edu

Abstract

The electrocatalytic reduction of carbon dioxide to hydrocarbons and oxygenates on Cu electrodes proceeds through surface-adsorbed CO. The adsorption and desorption of this intermediate play a key role in determining the product selectivity of this electrocatalytic process. It is therefore critical to understand the molecular factors that determine the adsorption of CO on Cu electrodes. In prior studies, it was suggested that specifically adsorbing anions of the supporting electrolyte compete with CO for surface sites at low overpotentials. However, prior infrared (IR) spectroscopy of CO adsorption on Cu electrodes did not compare the relative CO coverages in the presence of different anions and was restricted to a narrow range of electrolyte concentrations (0.1-0.2 M). Therefore, the impact of anions on the adsorption of CO on Cu is not fully understood to date. Herein, we systematically explored the adsorption and desorption of CO on polycrystalline Cu electrodes in the presence of specifically and non-specifically adsorbing anions (Cl^-, SO_4^{2-}, ClO_4^-) at two different concentrations (10 mM and 1 M) of the corresponding sodium salts. With surface-enhanced IR absorption spectroscopy (SEIRAS), we monitored the C≡O stretch band of atop-bound CO (CO_{atop}) and an infrared band of the hydration shells of interfacial anions as a function of electrode potential. We found that, at an electrolyte concentration of 10 mM, the adsorption and desorption of CO_{atop} are virtually independent of the identity of the anions. By contrast, at an electrolyte concentration of 1 M, the CO_{atop} coverage is significantly impacted by the electrolyte anions. The saturation coverages of CO_{atop} are lower in the 1 M electrolytes compared to those in the 10 mM electrolytes. The magnitude and mechanism of the modulation depends on the identity of the anions. Weakly and non-specifically adsorbing anions (SO_4^{2-}, ClO_4^-) limit the CO_{atop} saturation coverage by blocking a fraction of CO adsorption sites. However, their site-blocking ability depends on the CO coverage, as evidenced by the hysteresis in the CO adsorption/desorption profiles, which likely originates from a reversible CO-induced surface reconstruction. Chloride ions, which can specifically adsorb on Cu electrodes, lower the CO coverage by modulating the CO adsorption energy. This modulation manifests itself in (1) a distinctly higher C≡O stretch frequency in the presence of this anion relative to that measured in the other electrolytes and (2) the absence of the hysteresis in the adsorption/desorption profiles. Our study highlights the intricate interplay between anions and surface-adsorbed CO at the Cu electrode/electrolyte interface.

Introduction

Surface-adsorbed CO (CO_{ads}) is a key reaction intermediate in the reduction of CO_2 to hydrocarbons on Cu electrodes.[1–5] The ability of

Cu to reduce CO_{ads} to hydrocarbons at comparatively high reaction rates is attributable to the intermediate adsorption energy of CO on Cu relative to the adsorption energies on other pure metals.[6,7] For example, on the (111) facets of Au and Pt, the adsorption energies of atop-bound CO (CO_{atop}) are 0.04 and 1.45 eV, respectively.[8] As a result, the desorption of CO_{ads} is favored over its further reduction on Au, whereas CO_{ads} poisons the Pt surface under CO_2 reduction conditions.[6,7] By contrast, the binding energy of CO on Cu (0.62 eV for CO_{atop} on Cu(111)[8]) falls between these two values, giving rise to an intermediate CO coverage that permits co-adsorption of hydrogen,[7,9,10] thereby enabling the reduction of CO_{ads} at significant reaction rates (≈ 5 mA cm^{-2}).[6,11] However, the reduction of CO_2 to hydrocarbons on Cu requires a significant overpotential of ≈ 1 V and exhibits poor product selectivity.[6] To improve the catalytic activity and selectivity, it is essential to identify the molecular properties of the electrochemical interface that control the adsorption of CO on Cu at low overpotentials.

The adsorption energy can be tuned by altering the coordination of surface atoms through alloying or roughening of the surface.[12–17] However, for a given metal surface, the CO adsorption energy is not a fixed value, but sensitively depends on the CO surface coverage and the presence of co-adsorbates. For example, the adsorption energy of CO_{atop} on Pt(111) drops by about a factor of two when the coverage changes from 1/4 to one monolayer.[18] Similarly, co-adsorbates can profoundly affect CO adsorption energies and/or may block adsorption sites.[19–22] At an electrochemical interface, the binding energies of CO and co-adsorbates, and consequently the CO coverage, are functions of applied potential. Because the predominant co-adsorbates are species of the supporting electrolyte, altering the electrolyte composition presents an opportunity to tune the CO coverage, and therefore the catalytic activity and selectivity.

In earlier studies, specifically adsorbed anions of the supporting electrolyte were suggested to compete with CO for adsorption sites. It was shown that the cyclic voltammograms (CV) of Cu electrodes in electrolytes that contain anions that specifically adsorb exhibit redox waves in the presence of CO.[23–26] These redox waves were attributed to the displacement of specifically adsorbed anions from the surface upon adsorption of CO. This attribution is supported by the observations that the integrated C≡O stretch band area of CO_{atop} is (a) correlated with the integrated charge of the redox peak[23,24,26] and (b) anti-correlated with the integrated IR bands of interfacial phosphate[24] and carbonate[27,28] of the electrolyte with decreasing potential.

These pioneering studies established that the desorption of specifically adsorbing anions is correlated with the adsorption of CO on Cu. However, the relative CO coverages in the presence of different anions was not investigated in these earlier studies. Although the redox features in the CVs of Cu in the presence of CO were explored over a wide range of anions and electrolyte concentrations, the CO coverage as determined by infrared (IR) spectroscopy was only reported for a few select electrolytes (0.2 M phosphate,[24] 0.2 M perchlorate,[25] and 0.1-0.2 M carbonate[23,28]). A systematic comparison of the CO coverage on Cu electrodes as a function of different anions and their concentrations is still lacking to date. Moreover, with the exception of one study,[27] the CO coverage was only determined during the cathodic forward scans in these prior studies. However, the formation of a CO adlayer on the metal surface alters the properties of the metal/electrolyte interface.[3,29,30] How the proposed competition between CO and anions for adsorption sites is affected once an adlayer has formed has not been systematically investigated to date. In this work, we address these key questions.

Herein, we investigated how the identity and concentration of the electrolyte anion affect the adsorption of CO on polycrystalline Cu electrodes. With surface enhanced IR absorption spectroscopy (SEIRAS), we monitored the CO adsorption process on Cu electrodes in contact with 10 mM and 1 M aqueous solutions of $NaClO_4$, Na_2SO_4, and NaCl. We found that in the 10 mM electrolytes, the CO adsorption/desorption profiles as a function of

electrode potential are invariant with the identity of the supporting electrolyte's anion. In 1 M $NaClO_4$ and Na_2SO_4, the CO saturation coverage is about 2/3 of that in the corresponding dilute electrolytes. The lower coverage is indicative of the blocking of CO adsorption sites by quasi-specifically adsorbed anions. In all electrolytes but 1 M NaCl, we observed a pronounced hysteresis in the CO adsorption/desorption profiles. We attribute the higher stability of the CO adlayer on the anodic reverse scan to a reversible CO-driven surface reconstruction of the electrode. We propose that the absence of the hysteresis in 1 M NaCl is due to the co-adsorption of Cl^- anions, which decreases the CO adsorption energy. The co-adsorption manifests itself in the form of a markedly blue-shifted C≡O stretch frequency of CO_{atop} relative to that in the other electrolytes. Interestingly, the onset potentials for CO adsorption on Cu are similar for the different electrolytes. Taken together, our results show that while anions of the supporting electrolyte significantly impact the CO coverage on polycrystalline Cu, they have little effect on the onset potential of CO adsorption.

Methods

Materials. Sodium perchlorate hydrate (99.99% trace metals basis) and sodium chloride (99.999% trace metals basis) were sourced from Sigma-Aldrich. Sodium sulfate (99.9955% metals basis) was procured from Alfa Aesar Puratronic. D_2O (99.8 atom% D) from Acros Organics was used in all experiments. CO (ultra high purity) and Ar (ultra high purity) were obtained from Air Gas.

SEIRAS. SEIRAS experiments were carried out in a home-built two-compartment polyetheretherketone (PEEK) cell with the catholyte (6 ml) and anolyte (4 ml) separated by a Selemion AMV anion exchange membrane (AGC Engineering Co.; Chiba, Japan).[31] A graphite rod (99.995%; Sigma Aldrich) and an Ag/AgCl electrode (3 M NaCl; Basi Inc.; West Lafayette, IN) were used as the counter and reference electrodes, respectively. The catholyte was stirred at 900 rotations per minute (rpm) with a magnetic stir bar. The cell was connected to a nitrogen-purged attenuated total internal reflection (ATR) accessory (VeeMax III; Pike Technologies; Madison, WI) in the sample compartment of a Bruker Vertex 70 Fourier-transform infrared (FTIR) spectrometer, which was interfaced with a liquid nitrogen-cooled mercury cadmium telluride (MCT) detector (FTIR-16; Infrared Associates; Stuart, FL). The potential was controlled with a Versastat 3 potentiostat (AMETEK; Berwyn, PA). Further details on the spectroscopic procedures and the preparation of the chemically deposited thin films have been described in prior reports.[32,33] To clean the thin film electrode, the film was subjected to 5 CVs from −0.13 to −0.6 V versus Ag/AgCl at a scan rate of 50 mV s^{-1} under Ar purge at 5 standard cubic centimeter per minute (sccm). Following these cleaning CVs, the interfacial capacitance (Figure S1, SI) and solution resistance were measured. 85% of the solution resistance was compensated *in situ*. The remaining 15% was manually corrected following each experiment. To avoid potential complications due to Cu oxides and hydroxides,[34,35] a CV was carried out from −0.6 to −1.2 V versus Ag/AgCl at 10 mV s^{-1} to remove residual surface oxides and hydroxides. Following this CV, the cell was never returned to open circuit until completion of the experiment. To saturate the electrolyte with CO, the gas purge was then switched from Ar to CO. CO was purged for 20 min at a flow rate of 5 sccm while the potential was maintained at −0.6 V. Then, the spectroscopic measurements were carried out during the CVs from −0.6 to −1.4 V versus Ag/AgCl at a scan rate of 2 mV s^{-1}. CO was continuously purged until completion of the experiment.

Results and Discussion

Choice of Electrolytes. To explore how the adsorption of CO on polycrystalline Cu is impacted by different electrolyte anions, we monitored the Cu/electrolyte interface with SEIRAS in the ATR configuration. A chemically de-

posited Cu thin film on a Si ATR crystal served as the working electrode. We carried out all experiments in a two-compartment spectroelectrochemical cell under stirring of the electrolyte. As electrolytes, we employed aqueous solutions of $NaClO_4$, Na_2SO_4, and NaCl. We chose these anions because their interactions with the Cu surface are significantly different from each other, enabling us to probe how the anion-Cu interaction affects the adsorption of CO. Surface-enhanced spectroscopy studies found that ClO_4^- only physisorbs on Cu electrodes,[36] whereas SO_4^{2-} and Cl^- can specifically adsorb on Cu.[36–38] We used D_2O instead of H_2O as a solvent. Because of the kinetic isotope effect, the hydrogen evolution reaction in D_2O is slower by about one order of magnitude relative to the rate of the reaction in H_2O.[39] Therefore, the use of this solvent minimizes the Faradaic current during the spectroscopic study. Despite the suppression of the Faradaic current, the bulk pH of the unbuffered electrolytes drifted from $\approx$ 7.2 to $\approx$ 10.1 during the course of an experiment (Table S1, Supporting Information (SI)). Prior studies showed that the adsorption profiles of CO on Cu are essentially independent of the hydroxide concentration in this range.[2] As described below, we conducted control experiments to exclude pH effects on the findings of this study.

Impact of Anions on CO Adsorption. Figure 1 shows representative C≡O stretch spectra of CO_{atop} during CVs from −0.6 to −1.4 V versus Ag/AgCl in a 10 mM solution of $NaClO_4$. Unless otherwise noted, all potentials in this article are referenced against the Ag/AgCl electrode. The spectra in 10 mM solutions of Na_2SO_4 and NaCl are similar to the ones shown in Figure 1 (Figure S2, SI). The CVs were carried out at a scan rate of 2 mV s^{-1}, which is sufficiently slow to achieve a steady-state population of CO_{atop} on Cu.[2] The reversible changes in lineshape with applied potential were the topic of prior investigations and are attributed to a combination of reversible surface reconstruction and dynamical dipole coupling.[3,31] Integration of the band areas give a quantity that is approximately proportional to the CO surface coverage,[2,23,26] though dynamical dipole coupling may cause deviations from Beer's law at high coverage.[40]

Figure 2A shows the integrated C≡O stretch band areas of CO_{atop} during the CVs in 10 mM solutions of the salts. The reddish traces represent the forward scans and the bluish traces represent the reverse scans. The corresponding electrochemical current CVs are shown in Figure S3 of the SI. As shown, the integrated band areas are virtually independent of the identity of the anion. Further, the CVs exhibit a marked hysteresis between forward and reverse scans, with the reverse scan shifted to more anodic potentials by $\approx$ 95 mV. The hysteresis is also observed during a second consecutive CV (Figure S4, SI), demonstrating that the hysteretic behavior is due to a reversible interfacial process.

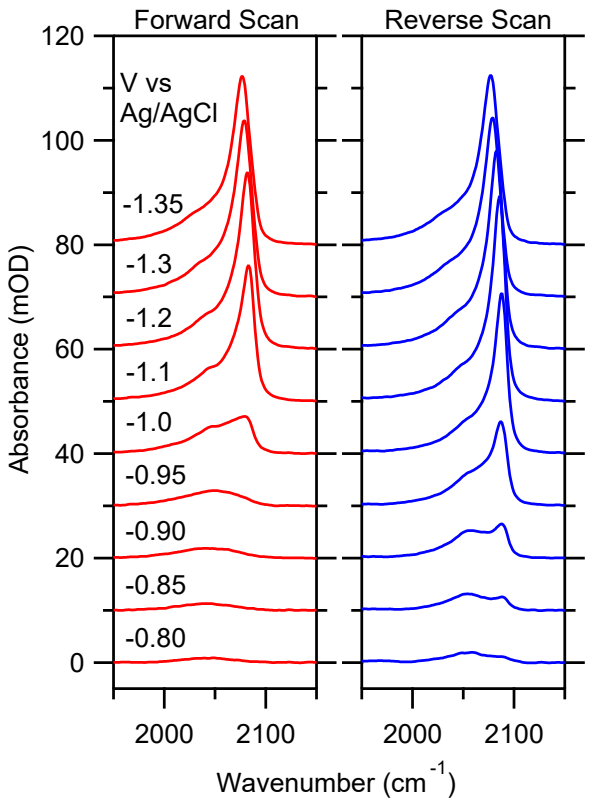

Figure 1: Representative C≡O stretch spectra of CO_{atop} on Cu as a function of applied potential during the cathodic forward (red) and anodic reverse scans (blue) in 10 mM $NaClO_4$ in D_2O. The reference potential was −0.6 V.

As shown in Figure 2B, in the 1 M electrolytes, the integrated C≡O stretch band areas

of CO_{atop} are affected by the anions in solution: First, the band areas at saturation coverage are $\approx 35\%$ lower in the presence of 1 M ClO_4^- and SO_4^{2-} compared to those at the saturation coverage in the corresponding 10 mM electrolytes. This observation suggests that ClO_4^- and SO_4^{2-} partially block CO adsorption sites. The CO_{atop} saturation coverage is attained at ≈ -1.3 V, which is about 0.4 V more negative that the potential of zero charge of polycrystalline Cu (-0.93 V in $NaClO_4$ under acidic pH conditions).[41] Therefore, at a potential of ≈ -1.3 V, the electrostatic force between anions and electrode is repulsive and consequently cannot be the origin of the apparent site-blocking effect. This observation suggests the existence of a direct or indirect chemical interaction between the anions and electrode. ClO_4^- and SO_4^{2-} are not expected to specifically adsorb on Cu electrodes in this potential range,[36] ruling out a direct chemical interaction.

It is probable that the interaction of anions with the electrode is mediated by other electrolyte species. At a potential of ≈ -1.3 V, Na^+ is the dominant charged species in the electric double layer. Density functional theory (DFT) studies showed that alkali metal cations can specifically adsorb on Cu and other metal electrodes at a potential of -1.3 V.[42,43] Surface-enhanced Raman spectroscopy (SERS) studies found that specifically adsorbed phosphate anions on Ag electrodes are more stable under cathodic polarization in the presence of Cs^+ than in K^+-containing electrolyte.[44] Cation-induced adsorption of persulfate anions on mercury electrodes was suggested as the reason for the accelerated reduction of this anion with increasing alkali metal cation concentration.[45] Taken together, we tentatively attribute the blocking effects to the presence of quasi-specifically adsorbed anions, that is, anions whose interaction with the electrode is mediated by Na^+.

We note that in a prior study, a more positive onset potential was reported for CO adsorption on Cu(100) in ClO_4^--containing electrolyte relative to that in electrolytes containing specifically adsorbing anions.[25] Analysis of Figure 2 reveals that the onset potential is between -0.65 and -0.7 V for polycrystalline Cu, regardless of cation identity and concentration. In this study, we define the onset potential for CO adsorption as the potential where the integrated band area reaches $\approx 1\%$ of the saturation coverage. The effects of anions and cations are well known to depend on the structure of the electrode surface.[46–48] Therefore, we attribute these diverging observations to the different electrode morphologies.

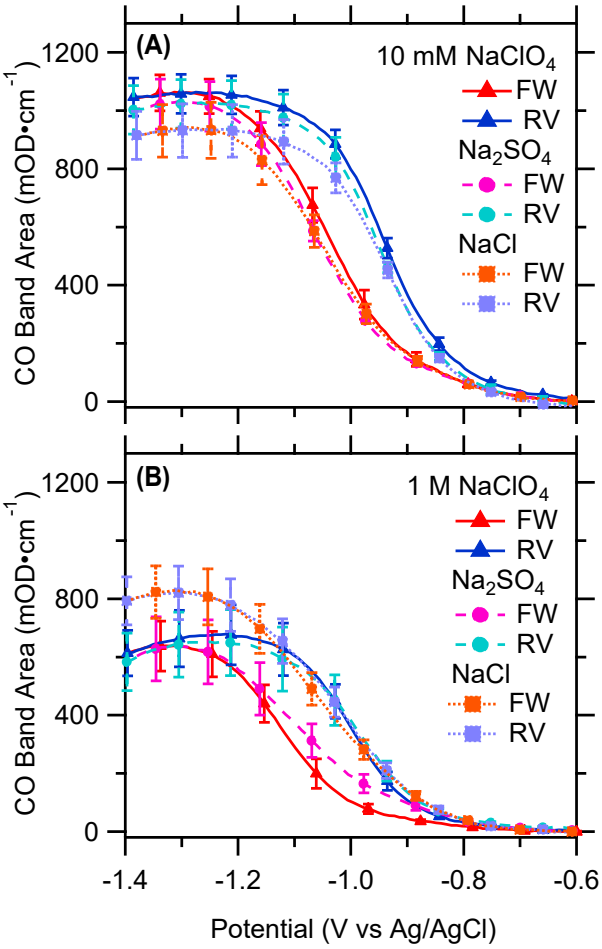

Figure 2: Integrated C≡O stretch band areas of CO_{atop} as a function of applied potential in (A) 10 mM and (B) 1 M electrolytes as indicated. Each trace is an average of a minimum of three experimental results. For each experiment, a fresh Cu film electrode was prepared. FW and RV denote forward and reverse scans, respectively. Error bars represent standard errors. For clarity, only a subset of the collected data points is shown.

Second, in the presence of 1 M Cl^-, the integrated band area at the CO saturation coverage

decreases by only $\approx 12\%$ compared to that in 10 mM NaCl. This result indicates that in contrast to the oxy-anions, Cl^- does not block CO adsorption sites to any significant extent.

Third, the hysteresis between forward and reverse scans that is apparent for all other electrolytes is absent for 1 M NaCl. The hysteresis could arise from reversible or irreversible processes at the interface. Irreversible changes at the interface include surface reconstructions of the electrode and an increase in interfacial pH due to hydrogen evolution. To test if irreversible changes cause the hysteresis, we conducted two consecutive CVs in 1 M Na_2SO_4. As in the experiment with 10 mM Na_2SO_4, the integrated C≡O stretch band areas of the first and second cycles closely overlap in 1 M Na_2SO_4 (Figure S4, SI). Further, the surface roughness of the electrodes before and after the CVs changed by $< 10\%$ for all 1 M electrolytes (Table S1 and Figure S1, SI). Taken together, these experiments indicate that no significant irreversible restructuring of the surface occurs during the CVs. The overlapping consecutive CVs suggest that the increase in pH during the experiments does not cause the hysteresis. This conclusion is further supported by the following prior findings: In pH-buffered electrolytes, similar degrees of hysteresis were observed in (a) the integrated C≡O stretch band areas of CO_{atop} on Cu and (b) the CV redox peaks due to charge displacement adsorption of CO on Cu.[2,24] Together with these prior findings, our results indicate that the hysteresis in the CO adsorption profiles is a more general feature of the Cu/electrolyte interface. Our observations indicate that the hysteresis is due to a reversible interfacial process, as discussed below.

Comparison of the traces for NaCl electrolytes in Figures 2A and B shows that the absence of the hysteresis in 1 M NaCl is mainly due to the shift of the anodic reverse scan to more cathodic potentials in that electrolyte. These observations raise two questions: (1) What is the origin of the hysteresis in the CVs? (2) Why is the hysteresis absent in 1 M Cl^-?

Origin of the Hysteresis. The hysteresis in the integrated C≡O stretch band areas of CO_{atop} could arise from a number of different reasons. For example, hysteretic behavior in the IR bands of an ionic liquid/electrode interface was attributed to an activation barrier associated with the rearrangement of interfacial charge as the electrode potential is altered.[49] In the present case, the CVs exhibit similar degrees of hysteresis for a broad range of different electrolytes. This observation suggests that electrolyte species are likely not the origin of the hysteresis. It is more probable that the formation of the CO_{atop} adlayer itself gives rise to the hysteretic behavior. Density functional theory (DFT) studies showed that the CO binding energy on metals is a strong function of the CO surface coverage.[7,18,50] For example, the chemisorption energy of CO_{atop} on Pt(100) drops from 1.80 to 1.16 eV as the coverage changes from 1/4 to one monolayer.[18] This decrease in binding energy is primarily due to repulsive interactions between nearest neighbor CO_{atop} molecules. For adlayers involving multiply bonded CO, bonding competition and electron delocalization can also substantially alter the binding energy.[18] For the vacuum/metal interface, the CO binding energy generally decreases with increasing coverage.[7,18,50] This predicted trend in binding energy contrasts with the observed higher stability of the CO_{atop} adlayer on the anodic reverse scans (Figure 2) in the present case. Though it is possible that the presence of the electrolyte alters the trends predicted by the DFT calculations of the vacuum/metal interface, it is more probable that effects other than an increase in CO coverage contribute to the hysteresis. Indeed, in these studies the structures of the metal surfaces were invariant with CO coverage. However, under many experimental conditions, the adsorption of CO is known to alter the surface structure.[51–54] As described below, a key contributor to the hysteresis is likely a CO-induced reconstruction of the electrode surface.

The adsorption of CO can induce morphological changes of metal surfaces.[51–54] For example, adsorption of CO on Cu(111) was shown to induce the formation of CO-stabilized Cu nanoclusters on the surface.[53] We previously showed that polycrystalline Cu electrodes undergo a reversible CO-driven reconstruction

that renders the surface more favorable for the adsorption of CO.[3] Specifically, with SEIRAS and SERS we demonstrated that the adsorption of CO induces a reversible reconstruction of the polycrystalline surface that brings about a higher density of undercoordinated Cu surface atoms that bind CO more strongly. Therefore, the CO-covered surface is expected to bind CO more strongly than the CO-free surface, which is consistent with the observed hysteresis. In agreement with this interpretation, at the gas/Pt(100) interface, hysteresis in the CO adsorption/desorption profiles as a function of temperature was attributed to a CO-induced reconstruction of the Pt surface.[51] Similarly, the presence of CO was found to impact a reversible surface reconstruction of Au(100) electrodes in alkaline electrolyte.[29] On the basis of these findings, we suggest that the hysteresis in the C≡O stretch band areas of CO_{atop} primarily arises from CO-induced reconstruction of the Cu surface.

Interplay of CO_{atop} and Anions. Because the chemisorption energy of CO_{atop} is coverage dependent, the formation of the CO_{atop} adlayer is expected to impact the interplay between CO_{atop} and interfacial anions. To gain a better understanding of this interplay, we monitored changes in the interfacial anion concentrations with applied potential. Because Cl^- cannot be observed with IR spectroscopy and because the vibrational modes of ClO_4^- and SO_4^{2-} are outside the experimentally accessible spectral window of our setup, we monitored the hydration shells of the anions. It is important to note that these measurements detect the depletion or enrichment of anions over the full width of the electric double layer as the potential is altered. The IR spectroscopic measurements of the hydration shells cannot differentiate between specifically adsorbed anions and anions in the double layer that are not in direct contact with the electrode.

Figure 3 shows the IR spectra in the 2500−2850 cm^{-1} region in the 1 M electrolytes and at a sample potential of −1.2 V (reference potential: −0.6 V). In this region, the potential-dependent spectral changes are due to the O−D stretch of interfacial D_2O. The spectrum exhibits a biphasic feature with a positive band at ≈ 2710 cm^{-1} and a negative band at ≈ 2660 cm^{-1}. The band at ≈ 2710 cm^{-1} is attributable to interfacial water in direct contact with surface-adsorbed CO, as demonstrated in an earlier publication.[33] The IR spectrum of the bulk $NaClO_4$ solution also exhibits a band at ≈ 2660 cm^{-1} (Figure S5, SI). Earlier studies demonstrated that this band is due to water in the hydration shells of the anions.[55,56] Therefore, the negative peak at ≈ 2660 cm^{-1} arises from the displacement of anions from the interface with decreasing electrode potential. We note that the 2660 cm^{-1} band may not be purely due to the hydration shells of anions. In the case of NaCl, it may indicate the solvation of surface-adsorbed $Cl^{\delta-}/Na^+$ pairs.[57] We note that this band was not observable in the 10 mM electrolytes because of the low concentration of anions. To obtain the integrated area of the 2660 cm^{-1} band, we modeled the spectra in the 2500−2850 cm^{-1} region with a set of two Gaussian functions and a linear background. The potential-dependence of representative spectra and the corresponding fits are shown in Figure S6 of the SI.

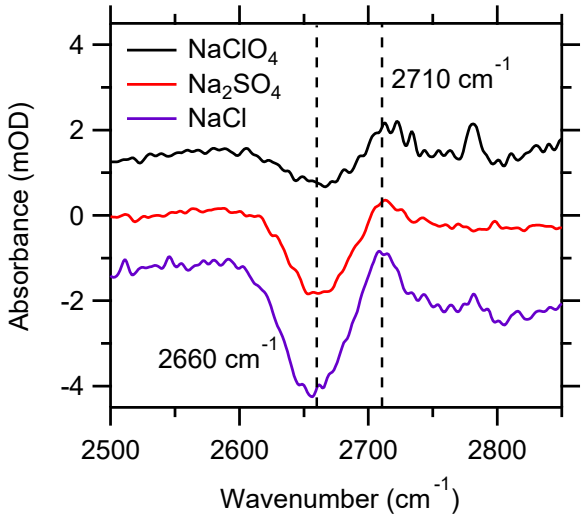

Figure 3: Representative O−D stretch spectra at a potential of −1.2 V in the 1 M electrolytes as indicated. The reference potential was −0.6 V.

Figure 4 shows the normalized 2660 cm^{-1} band area (right y-axis, dashed lines) together

with the normalized C≡O stretch band area (left y-axis, solid lines) as a function of potential for each electrolyte. For easier interpretation, we normalized the band areas at the cathodic turning potential of the CVs. The unnormalized integrated areas of the 2660 cm^{-1} band are shown in Figure S7 of the SI. Prior studies found that the adsorption of CO on polycrystalline Cu electrodes is correlated with the desorption of specifically adsorbed phosphate and carbonate anions.[24,27,28] In comparison to these earlier studies, Figure 4 reveals a more nuanced picture of the interplay between CO_{atop} and interfacial anions. Similar to prior observations with phosphate and carbonate,[24,27,28] the decrease in the integrated 2660 cm^{-1} band in the presence of ClO_4^- and Cl^- during the cathodic forward scan closely correlates with the rise of the integrated C≡O stretch band area (Figure 4A,C). The corresponding band for SO_4^{2-} declines at potentials more positive than −0.9 V (Figure 4B), supposedly because of the higher charge density of SO_4^{2-} compared to the other two anions.

During the anodic reverse scan, ClO_4^- and SO_4^{2-} return to the interface at a steeper rate compared to the rate of depletion during the respective cathodic branch of the CV. Like the hysteresis in the C≡O stretch band area, the hysteresis of the 2660 cm^{-1} band area also occurs during a second consecutive CV (Figure S8, SI). Despite this steeper rate in the return of ClO_4^- and SO_4^{2-}, the formed CO_{atop} adlayer is stable at more anodic potentials relative to the adlayer during the cathodic scan. This observation indicates that the stabilization of the CO_{atop} adlayer by CO-induced surface reconstruction is sufficiently strong to prevent the disruption of the adlayer by ClO_4^- and SO_4^{2-} as the potential is tuned more positively.

In the presence of Cl^-, there is essentially no hysteresis in the integrated 2660 cm^{-1} band area (Figure 4C). Further, the decline of this band area is closely correlated with the rise of the C≡O stretch band area. These observations suggest that the adsorption of CO is influenced by Cl^-.

Interaction of CO_{atop} and Cl^-. To investigate the interaction between CO_{atop} and

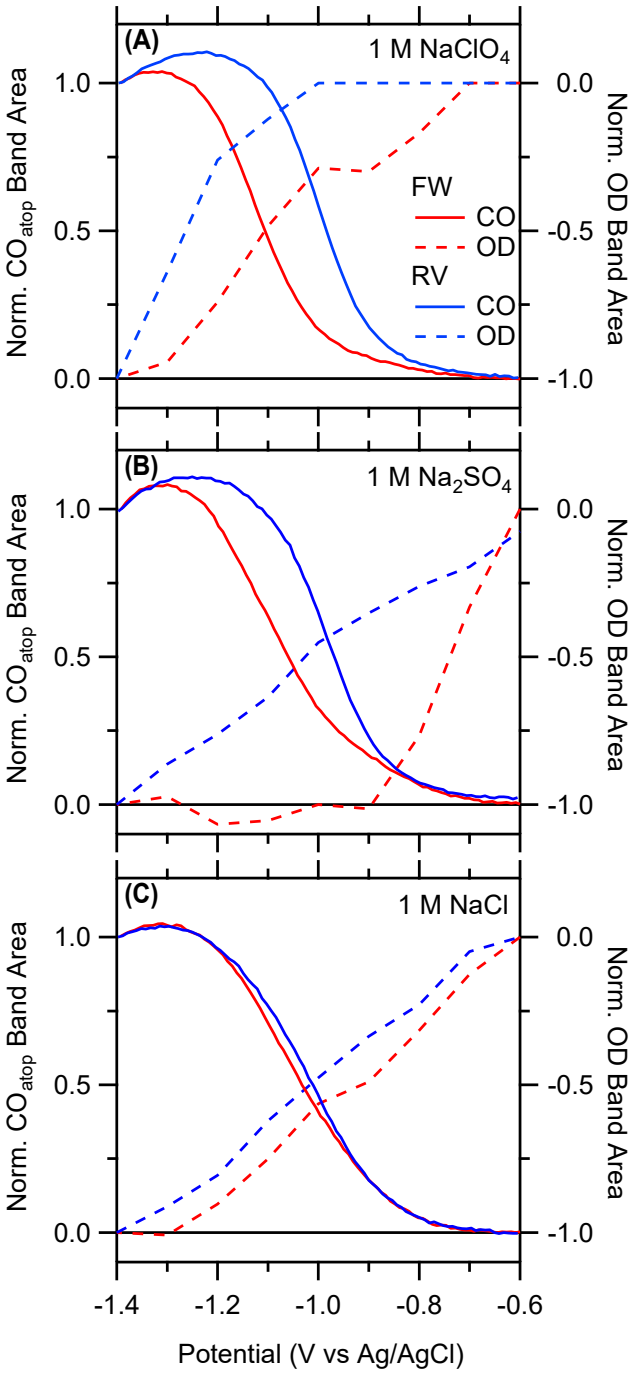

Figure 4: Normalized areas of the 2660 cm^{-1} O−D stretch band (right y-axis) and C≡O stretch band (left y-axis) as a function of applied potential in 1 M solutions of (A) $NaClO_4$, (B) Na_2SO_4, and (C) NaCl.

Cl^-, we analyzed the peak frequencies of the C≡O stretch band in the presence of the different electrolytes. We restricted this analysis to potentials ≥ -0.85 V, where the CO_{atop} coverage is low and frequency shifts due to dynamical dipole coupling are expected to be minimal.[31,58] Representative C≡O stretch spectra of CO_{atop} at a potential of -0.85 V and the corresponding Gaussian fits are shown in Figure S9 of the SI. In the 10 mM electrolytes, the C≡O stretch frequencies in the presence of different anions are very similar to each other (within ≈ 5 cm^{-1}, Figure S10, SI). Figure 5 shows the potential-dependence of the frequency in 10 mM $NaClO_4$ as a reference. Relative to this reference, the stretch frequency in 1 M $NaClO_4$ is very similar. Whereas the stretch frequency in the presence of SO_4^{2-} shows a moderate blue-shift of ≈ 5 cm^{-1} relative to that in 10 mM $NaClO_4$, the frequency in the presence of 1 M Cl^- is strongly blue-shifted by ≈ 19 cm^{-1}. This trend in the C≡O stretch frequency follows the trend of increasing tendency of the anion to specifically adsorb on the Cu electrode ($ClO_4^- < SO_4^{2-} < Cl^-$).[36,37] These results further corroborate that specifically adsorbed Cl^- ions alter the interaction of CO with the Cu surface.

As discussed above, at more cathodic potentials (< -0.85 V), SO_4^{2-} and ClO_4^- are expected to be quasi-specifically adsorbed on the electrode. Therefore, the lower CO_{atop} saturation coverage in the presence of 1 M of these anions (Figure 2) is not due to the modulation of the CO adsorption energy but a result of the blocking of CO adsorption sites by these anions.

We note that the C≡O stretch frequency decreases as the potential is tuned more cathodically (Figure 5). This change in frequency with applied potential is due to the vibrational Stark effect, which describes the effect of the interfacial electric field on the vibrational mode.[33,59,60] Therefore, this shift is primarily attributable to an electric double layer effect rather than a change in surface bonding with coverage and/or potential. The rate at which the frequency is changing with potential is similar for the 1 M electrolytes (Figure 5), indicating that the change in the interfacial electric field with potential is similar for the three different electrolytes.

At the vacuum/metal interface, some co-adsorbates were shown to impact the binding energy and C≡O stretch frequency of adsorbed CO.[19,20] Although such "ligand effects" can arise from various different mechanisms, they were often successfully interpreted in terms of the distribution of surface charge among the co-adsorbates and adsorbed CO molecules. In the present case, the blue shift of the C≡O stretch mode is suggestive of bonding competition between CO_{atop} and specifically adsorbed Cl^-. That is, less charge donation from the metal to the π^* orbital of CO_{atop} occurs compared to the absence of specifically adsorbed Cl^-. A lesser degree of charge back-donation to the π^* orbital of CO_{atop} is expected to blue-shift the C≡O stretch frequency,[20] consistent with the observations in Figure 5.

Less back-donation to the π^* orbital of CO_{atop} is expected to lower the binding energy of CO to the Cu surface.[61] Indeed, DFT calculations showed that the co-adsorption of I^- on Cu weakens the CO binding energy by 0.07 to 0.33 eV, depending on the crystallographic facet.[43] A smaller binding energy of CO_{atop} lowers the propensity of the surface to reconstruct upon CO adsorption, consistent with the observation that the hysteresis is absent in 1 M NaCl electrolyte (Figures 2 and 4C). The modulation of the CO_{atop} binding energy by Cl^- may partially explain the dependence of the product selectivity and/or rate of CO_2 reduction on the identity of the supporting electrolyte's halide anion.[62–65]

We note that prior experimental[66–68] and computational[38,69,70] studies found that Cl^- desorbs from Cu electrodes at potentials more negative than ≈ -0.56 to -0.88 V versus Ag/AgCl, depending on the crystallographic facet and surface coverage. The prior experimental studies were typically carried out at low Cl^- concentrations in the electrolyte. At a Cl^- concentration of 1 M, a low coverage of Cl^- on the Cu electrode is expected at much more negative potentials. This assertion is supported by recent work[62] that showed that (a) small amounts of Cl^- remain on the Cu surface after 1 h of CO_2 reduction in 0.1 M $KHCO_3$ + 0.3 M KCl at a potential of -1.0 V versus

the reversible hydrogen electrode, and (b) the magnitude of the reduction current at the same potential is linearly correlated with the DFT-calculated adsorption potential of the halide in the electrolyte. Further, enhancements of the reduction of CO_2 that are not only due to halide-induced surface restructuring have been reported for a number of differently prepared Cu electrodes.[63–65,71,72] These results confirm our notion that at the most cathodic potential employed in our work (−1.4 V), the Cl^- coverage on the electrode is sufficiently high to alter the CO_{atop} binding energy.

Irreversibly Adsorbed Species. In the course of the CVs, we observed two irreversible changes in the spectra. First, a weak IR band due to bridge-bonded CO (CO_{bridge}) appears in the CVs (Figure S11, SI). The band is most pronounced in 1 M NaCl. As demonstrated in an earlier publication, this low coverage of CO_{bridge} does not measurably impact the binding of CO_{atop}.[32] Second, during the anodic reverse scans, the O−D stretch band of D_2O increases (Figure S6, SI). In a prior study, the appearance of this band was attributed to the adsorption of water on Cu.[2] Our control experiments of two consecutive CV cycles (Figure S4, SI) demonstrate that this process does not significantly impact the binding of CO_{atop}.

Conclusions

Herein, we investigated to what extent anions of the supporting electrolyte affect the adsorption of CO_{atop} on Cu electrodes. To this end, we studied the adsorption process in aqueous solutions of 10 mM and 1 M $NaClO_4$, Na_2SO_4, and NaCl. We found that, at low concentrations of anions (10 mM), the adsorption and desorption of CO_{atop} are virtually independent of the identity of the anion. By contrast, in 1 M electrolytes, the saturation coverage of CO_{atop} depends on the anion type. Interestingly, we found that weakly and non-specifically adsorbing anions (ClO_4^- and SO_4^{2-}) limit the CO_{atop} saturation coverage. This observation suggests that quasi-specifically adsorbed anions block a fraction of CO adsorption sites. However, their

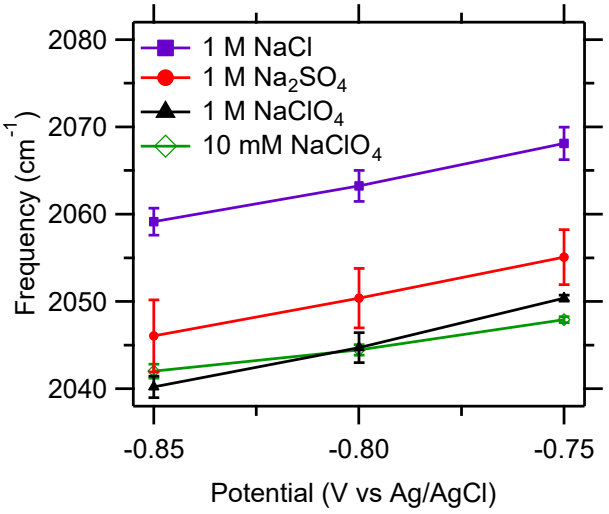

Figure 5: Peak frequencies of the C≡O stretch band as function of applied potential at low CO_{atop} coverage. Each trace is an average of a minimum of three independent experimental results. Error bars represent standard errors.

ability to do so depends on the absolute CO_{atop} coverage, as indicated by the pronounced hysteresis of the adsorption/desorption profiles of CO and depletion/enrichment profiles of interfacial anions. We attribute the higher stability of the CO_{atop} adlayer in part to a reversible CO-driven reconstruction of the Cu surface, as reported in one of our prior studies.[3] By contrast, in 1 M NaCl, there is virtually no hysteresis in the adsorption/desorption profile of CO_{atop} and depletion/enrichment profile of hydrated Cl^- anion at the interface. Further, the profiles of the two species are closely correlated, suggesting that specifically adsorbed Cl^- affects the chemisorption of CO_{atop} on the Cu electrode. As evidenced by the distinctly blue-shifted C≡O stretch frequency of CO_{atop} in 1 M NaCl relative to those in the other electrolytes, the chemisorption of CO_{atop} is weakened by specifically adsorbed Cl^-. This weaker interaction between CO and Cu is consistent with a lower ability of CO_{atop} to induced surface reconstruction and the resulting absence of the hysteresis in the adsorption/desorption profiles in 1 M NaCl. Our study shows that anions play an important role in the chemisorption of CO on Cu electrodes. However, the onset potential of CO adsorption is surprisingly insensitive to

anion identity and concentration. Therefore, to shift the adsorption profile of CO on polycrystalline Cu to more anodic potentials, strategies other than changing the electrolyte anion are likely more effective.

Acknowledgement This work was supported by a CAREER award from the National Science Foundation (Award No.: CHE-1847841).

Supporting Information Available

Representative CVs for thin film roughness characterization. Representative potential-dependent IR spectra of CO_{atop} in 10 mM $NaClO_4$ and Na_2SO_4. Electrical current density CVs in 10 mM and 1 M electrolytes. Integrated C≡O stretch band areas of CO_{atop} during consecutive CVs in 10 mM and 1 M Na_2SO_4. IR spectra of solution phase 1 M $NaClO_4$. Representative potential-dependent IR spectra of interfacial D_2O with Gaussian fittings of the 2660 and 2710 cm^{-1} bands. Average unnormalized integrated 2660 cm^{-1} band areas. Integrated 2660 cm^{-1} band areas for consecutive CVs in 1 M Na_2SO_4. IR spectra of CO_{atop} in 1 M electrolytes at low coverage. Potential-dependent C≡O stretch peak frequencies in 10 mM electrolytes. Representative potential-dependent IR spectra of CO_{bridge} in 1 M electrolytes. Electrode roughness and electrolyte pH values before and after spectroscopic measurements.

References

(1) Hori, Y.; Murata, A.; Yoshinami, Y. Adsorption of CO, Intermediately Formed in Electrochemical Reduction of CO_2, at a Copper Electrode. *J. Chem. Soc., Faraday Trans.* **1991**, *87*, 125–128.

(2) Wuttig, A.; Liu, C.; Peng, Q.; Yaguchi, M.; Hendon, C. H.; Motobayashi, K.; Ye, S.; Osawa, M.; Surendranath, Y. Tracking a Common Surface-Bound Intermediate During CO_2-to-Fuels Catalysis. *ACS Cent. Sci.* **2016**, *2*, 522–528.

(3) Gunathunge, C. M.; Li, X.; Li, J.; Hicks, R. P.; Ovalle, V. J.; Waegele, M. M. Spectroscopic Observation of Reversible Surface Reconstruction of Copper Electrodes Under CO_2 Reduction. *J. Phys. Chem. C* **2017**, *121*, 12337–12344.

(4) Huang, Y.; Handoko, A. D.; Hirunsit, P.; Yeo, B. S. Electrochemical Reduction of CO_2 Using Copper Single-Crystal Surfaces: Effects of CO* Coverage on the Selective Formation of Ethylene. *ACS Catal.* **2017**, *7*, 1749–1756.

(5) Li, J.; Wang, Z.; McCallum, C.; Xu, Y.; Li, F.; Wang, Y.; Gabardo, C. M.; Dinh, C.-T.; Zhuang, T.-T.; Wang, L. et al. Constraining CO Coverage on Copper Promotes High-efficiency Ethylene Electroproduction. *Nat. Catal.* **2019**, *2*, 1124–1131.

(6) Kuhl, K. P.; Hatsukade, T.; Cave, E. R.; Abram, D. N.; Kibsgaard, J.; Jaramillo, T. F. Electrocatalytic Conversion of Carbon Dioxide to Methane and Methanol on Transition Metal Surfaces. *J. Am. Chem. Soc.* **2014**, *136*, 14107–14113.

(7) Akhade, S. A.; Luo, W.; Nie, X.; Bernstein, N. J.; Asthagiri, A.; Janik, M. J. Poisoning Effect of Adsorbed CO During CO_2 Electroreduction on Late Transition Metals. *Phys. Chem. Chem. Phys.* **2014**, *16*, 20429–20435.

(8) Hammer, B.; Morikawa, Y.; Nørskov, J. K. CO Chemisorption at Metal Surfaces and Overlayers. *Phys. Rev. Lett.* **1996**, *76*, 2141–2144.

(9) Heyes, J.; Dunwell, M.; Xu, B. CO_2 Reduction on Cu at Low Overpotentials with Surface-Enhanced in Situ Spectroscopy. *J. Phys. Chem. C* **2016**, *120*, 17334–17341.

(10) Schreier, M.; Yoon, Y.; Jackson, M. N.; Surendranath, Y. Competition between H

and CO for Active Sites Governs Copper-Mediated Electrosynthesis of Hydrocarbon Fuels. *Angew. Chem. Int. Ed.* **2018**, *57*, 10221–10225.

(11) Hori, Y.; Kikuchi, K.; Murata, A.; Suzuki, S. Production of CO and CH_4 in Electrochemical Reduction of CO_2 at Metal Electrodes in Aqueous Hydrogencarbonate Solution. *Chem. Lett.* **1985**, *14*, 1695–1698.

(12) Verdaguer-Casadevall, A.; Li, C. W.; Johansson, T. P.; Scott, S. B.; McKeown, J. T.; Kumar, M.; Stephens, I. E. L.; Kanan, M. W.; Chorkendorff, I. Probing the Active Surface Sites for CO Reduction on Oxide-Derived Copper Electrocatalysts. *J. Am. Chem. Soc.* **2015**, *137*, 9808–9811.

(13) Ross, M. B.; Dinh, C. T.; Li, Y.; Kim, D.; De Luna, P.; Sargent, E. H.; Yang, P. Tunable Cu Enrichment Enables Designer Syngas Electrosynthesis from CO_2. *J. Am. Chem. Soc.* **2017**, *139*, 9359–9363.

(14) Hoang, T. T. H.; Verma, S.; Ma, S.; Fister, T. T.; Timoshenko, J.; Frenkel, A. I.; Kenis, P. J. A.; Gewirth, A. A. Nanoporous Copper–Silver Alloys by Additive-Controlled Electrodeposition for the Selective Electroreduction of CO_2 to Ethylene and Ethanol. *J. Am. Chem. Soc.* **2018**, *140*, 5791–5797.

(15) Chen, X.; Henckel, D.; Nwabara, U.; Li, Y.; Frenkel, A. I.; Fister, T. T.; Kenis, P. J. A.; Gewirth, A. A. Controlling Speciation during CO_2 Reduction on Cu-Alloy Electrodes. *ACS Catal.* **2020**, *10*, 672–682.

(16) Malkani, A. S.; Dunwell, M.; Xu, B. Operando Spectroscopic Investigations of Copper and Oxide-Derived Copper Catalysts for Electrochemical CO Reduction. *ACS Catal.* **2019**, *9*, 474–478.

(17) Jiang, K.; Huang, Y.; Zeng, G.; Toma, F. M.; Goddard, W. A.; Bell, A. T. Effects of Surface Roughness on the Electrochemical Reduction of CO_2 over Cu. *ACS Energy Lett.* **2020**, *5*, 1206–1214.

(18) Mason, S. E.; Grinberg, I.; Rappe, A. M. Adsorbate-Adsorbate Interactions and Chemisorption at Different Coverages Studied by Accurate ab initio Calculations: CO on Transition Metal Surfaces. *J. Phys. Chem. B* **2006**, *110*, 3816–3822.

(19) Garfunkel, E. L.; Crowell, J. E.; Somorjai, G. A. The Strong Influence of Potassium on the Adsorption of Carbon Monoxide on Platinum Surfaces: a TDS and HREELS Study. *J. Phys. Chem.* **1982**, *86*, 310–313.

(20) Rodriguez, J. A.; Campbell, C. T. Quantum Chemical Studies of the Effects of Electron-transferring Ligands Upon Carbon Monoxide Chemisorption on Copper(100). *J. Phys. Chem.* **1987**, *91*, 2161–2171.

(21) Ovalle, V. J.; Waegele, M. M. Understanding the Impact of N-Arylpyridinium Ions on the Selectivity of CO_2 Reduction at the Cu/Electrolyte Interface. *J. of Phys. Chem. C* **2019**, *123*, 24453–24460.

(22) Li, F.; Thevenon, A.; Rosas-Hernandez, A.; Wang, Z.; Li, Y.; Gabardo, C. M.; Ozden, A.; Dinh, C. T.; Li, J.; Wang, Y. et al. Molecular Tuning of CO_2-to-Ethylene Conversion. *Nature* **2019**, *577*, 509–513.

(23) Hori, Y.; Koga, O.; Yamazaki, H.; Matsuo, T. Infrared Spectroscopy of Adsorbed CO and Intermediate Species in Electrochemical Reduction of CO_2 to Hydrocarbons on a Cu Electrode. *Electrochim. Acta* **1995**, *40*, 2617–2622.

(24) Hori, Y.; Koga, O.; Watanabe, Y.; Matsuo, T. FTIR Measurements of Charge Displacement Adsorption of CO on Poly- and Single Crystal (100) of Cu Electrodes. *Electrochim. Acta* **1998**, *44*, 1389–1395.

(25) Koga, O.; Watanabe, Y.; Tanizaki, M.; Hori, Y. Specific Adsorption of Anions on a Copper (100) Single Crystal Electrode Studied by Charge Displacement by CO Adsorption and Infrared Spectroscopy. *Electrochim. Acta* **2001**, *46*, 3083 – 3090.

(26) Koga, O.; Teruya, S.; Matsuda, K.; Minami, M.; Hoshi, N.; Hori, Y. Infrared Spectroscopic and Voltammetric Study of Adsorbed CO on Stepped Surfaces of Copper Monocrystalline Electrodes. *Electrochim. Acta* **2005**, *50*, 2475–2485.

(27) Sartin, M. M.; Yu, Z.; Chen, W.; He, F.; Sun, Z.; Chen, Y.-X.; Huang, W. Effect of Particle Shape and Electrolyte Cation on CO Adsorption to Copper Oxide Nanoparticle Electrocatalysts. *J. Phys. Chem. C* **2018**, *122*, 26489–26498.

(28) Wuttig, A.; Ryu, J.; Surendranath, Y. Electrolyte Competition Controls Surface Binding of CO Intermediates to CO_2 Reduction Catalysts. ChemRxiv, Preprint, 2019. `https://doi.org/10.26434/chemrxiv.7929038.v2`.

(29) Blizanac, B. B.; Lucas, C. A.; Gallagher, M. E.; Arenz, M.; Ross, P. N.; Marković, N. M. Anion Adsorption, CO Oxidation, and Oxygen Reduction Reaction on a Au(100) Surface: The pH Effect. *J. Phys. Chem. B* **2004**, *108*, 625–634.

(30) Sundararaman, R.; Figueiredo, M. C.; Koper, M. T. M.; Schwarz, K. A. Electrochemical Capacitance of CO-Terminated Pt(111) Dominated by the CO-Solvent Gap. *J. Phys. Chem. Lett.* **2017**, *8*, 5344–5348.

(31) Gunathunge, C. M.; Li, J.; Li, X.; Hong, J. J.; Waegele, M. M. Revealing the Predominant Surface Facets of Rough Cu Electrodes under Electrochemical Conditions. *ACS Catal.* **2020**, *10*, 6908–6923.

(32) Gunathunge, C. M.; Ovalle, V. J.; Li, Y.; Janik, M. J.; Waegele, M. M. Existence of an Electrochemically Inert CO Population on Cu Electrodes in Alkaline pH. *ACS Catal.* **2018**, *8*, 7507–7516.

(33) Li, J.; Li, X.; Gunathunge, C. M.; Waegele, M. M. Hydrogen Bonding Steers the Product Selectivity of Electrocatalytic CO Reduction. *Proc. Natl. Acad. Sci. USA* **2019**, *116*, 9220–9229.

(34) Iijima, G.; Inomata, T.; Yamaguchi, H.; Ito, M.; Masuda, H. Role of a Hydroxide Layer on Cu Electrodes in Electrochemical CO_2 Reduction. *ACS Catal.* **2019**, *9*, 6305–6319.

(35) Zhao, Y.; Chang, X.; Malkani, A. S.; Yang, X.; Thompson, L.; Jiao, F.; Xu, B. Speciation of Cu Surfaces During the Electrochemical CO Reduction Reaction. *J. Am. Chem. Soc.* **2020**, *142*, 9735–9743.

(36) Niaura, G.; Malinauskas, A. Surface-enhanced Raman Spectroscopy of ClO_4^- and SO_4^{2-} Anions Adsorbed at a Cu Electrode. *J. Chem. Soc., Faraday Trans.* **1998**, *94*, 2205–2211.

(37) Brown, G.; Hope, G. A SERS Study of SO_4^{2-}/Cl^- Ion Adsorption at a Copper Electrode In-Situ. *J. Electroanal. Chem.* **1996**, *405*, 211 – 216.

(38) Bagger, A.; Arán-Ais, R. M.; Halldin Stenlid, J.; Campos dos Santos, E.; Arnarson, L.; Degn Jensen, K.; Escudero-Escribano, M.; Cuenya, B. R.; Rossmeisl, J. Ab Initio Cyclic Voltammetry on Cu (111), Cu (100) and Cu (110) in Acidic, Neutral and Alkaline Solutions. *ChemPhysChem* **2019**, *20*, 3096–3105.

(39) Conway, B. E. Kinetics of Electrolytic Hydrogen and Deuterium Evolution. *Proc. R. Soc. London, Ser. A* **1960**, *256*, 128–144.

(40) Borguet, E.; Dai, H. Site-specific Properties and Dynamical Dipole Coupling of CO Molecules Adsorbed on a Vicinal Cu(100) Surface. *J. Chem. Phys.* **1994**, *101*, 9080–9095.

(41) Łukomska, A.; Sobkowski, J. Potential of Zero Charge of Monocrystalline Copper Electrodes in Perchlorate Solutions. *J. Electroanal. Chem.* **2004**, *567*, 95–102.

(42) Mills, J. N.; McCrum, I. T.; Janik, M. J. Alkali Cation Specific Adsorption onto fcc(111) Transition Metal Electrodes. *Phys. Chem. Chem. Phys.* **2014**, *16*, 13699–13707.

(43) Akhade, S. A.; McCrum, I. T.; Janik, M. J. The Impact of Specifically Adsorbed Ions on the Copper-Catalyzed Electroreduction of CO_2. *J. Electrochem. Soc.* **2016**, *163*, F477–F484.

(44) Niaura, G.; Jakubenas, R. The Alkali Metal Cation Effect on the Surface-enhanced Raman Spectra of Phosphate Anions Adsorbed at Silver Electrodes. *J. Electroanal. Chem.* **2001**, *510*, 50 – 58.

(45) Frumkin, A. N. Influence of Cation Adsorption on the Kinetics of Electrode Processes. *Trans. Faraday Soc.* **1959**, *55*, 156–167.

(46) Mostany, J.; Herrero, E.; Feliu, J. M.; Lipkowski, J. Thermodynamic Studies of Anion Adsorption at Stepped Platinum(hkl) Electrode Surfaces in Sulfuric Acid Solutions. *J. Phys. Chem. B* **2002**, *106*, 12787–12796.

(47) Pérez-Gallent, E.; Marcandalli, G.; Figueiredo, M. C.; Calle-Vallejo, F.; Koper, M. T. M. Structure- and Potential-Dependent Cation Effects on CO Reduction at Copper Single-Crystal Electrodes. *J. Am. Chem. Soc.* **2017**, *139*, 16412–16419.

(48) Waegele, M. M.; Gunathunge, C. M.; Li, J.; Li, X. How Cations Affect the Electric Double Layer and the Rates and Selectivity of Electrocatalytic Processes. *J. Chem. Phys.* **2019**, *151*, 160902.

(49) Motobayashi, K.; Minami, K.; Nishi, N.; Sakka, T.; Osawa, M. Hysteresis of Potential-Dependent Changes in Ion Density and Structure of an Ionic Liquid on a Gold Electrode: In Situ Observation by Surface-Enhanced Infrared Absorption Spectroscopy. *J. Phys. Chem. Lett.* **2013**, *4*, 3110–3114.

(50) Shi, C.; Hansen, H. A.; Lausche, A. C.; Nørskov, J. K. Trends in Electrochemical CO_2 Reduction Activity for Open and Close-Packed Metal Surfaces. *Phys. Chem. Chem. Phys.* **2014**, *16*, 4720–4727.

(51) Jackman, T. E.; Griffiths, K.; Davies, J. A.; Norton, P. R. Absolute Coverages and Hysteresis Phenomena Associated with the CO-induced Pt(100) hex$\leftrightarrow$(1$\times$1) Phase Transition. *J. Chem. Phys.* **1983**, *79*, 3529–3533.

(52) Zou, S.; Gomez, R.; Weaver, M. J. Infrared Spectroscopy of Carbon Monoxide at the Ordered Palladium (110)-Aqueous Interface: Evidence for Adsorbate-Induced Surface Reconstruction. *Surf. Sci.* **1998**, *399*, 270–283.

(53) Eren, B.; Zherebetskyy, D.; Patera, L. L.; Wu, C. H.; Bluhm, H.; Africh, C.; Wang, L.-W.; Somorjai, G. A.; Salmeron, M. Activation of Cu(111) Surface by Decomposition into Nanoclusters Driven by CO Adsorption. *Science* **2016**, *351*, 475–478.

(54) Gunathunge, C. M.; Ovalle, V. J.; Waegele, M. M. Probing Promoting Effects of Alkali Cations on the Reduction of CO at the Aqueous Electrolyte/Copper Interface. *Phys. Chem. Chem. Phys.* **2017**, *19*, 30166–30172.

(55) Bergstroem, P. A.; Lindgren, J.; Kristiansson, O. An IR Study of the Hydration of Perchlorate, Nitrate, Iodide, Bromide, Chloride and Sulfate Anions in Aqueous Solution. *J. Phys. Chem.* **1991**, *95*, 8575–8580.

(56) Kitamura, F.; Ohsaka, T.; Tokuda, K. Infrared Spectroscopic Observation

of Water at a Polycrystalline Gold Electrode|Aqueous Halide Solution Interface. *J. Electroanal. Chem.* **1996**, *412*, 183 – 188.

(57) Villegas, I.; Weaver, M. J. Infrared Spectroscopy of Model Electrochemical Interfaces in Ultrahigh Vacuum: Evidence for Coupled Cation-Anion Hydration in the Pt(111)/K^+,Cl^- System. *J. Phys. Chem.* **1996**, *100*, 19502–19511.

(58) Hollins, P.; Pritchard, J. Infrared Studies of Chemisorbed Layers on Single Crystals. *Prog. Surf. Sci.* **1985**, *19*, 275–349.

(59) Ge, A.; Videla, P. E.; Lee, G. L.; Rudshteyn, B.; Song, J.; Kubiak, C. P.; Batista, V. S.; Lian, T. Interfacial Structure and Electric Field Probed by in Situ Electrochemical Vibrational Stark Effect Spectroscopy and Computational Modeling. *J. Phys. Chem. C* **2017**, *121*, 18674–18682.

(60) Patrow, J. G.; Sorenson, S. A.; Dawlaty, J. M. Direct Spectroscopic Measurement of Interfacial Electric Fields near an Electrode under Polarizing or Current-Carrying Conditions. *J. Phys. Chem. C* **2017**, *121*, 11585–11592.

(61) Blyholder, G. Molecular Orbital View of Chemisorbed Carbon Monoxide. *J. Phys. Chem.* **1964**, *68*, 2772–2777.

(62) Gao, D.; Scholten, F.; Cuenya, B. R. Improved CO_2 Electroreduction Performance on Plasma-Activated Cu Catalysts via Electrolyte Design: Halide Effect. *ACS Catal.* **2017**, *7*, 5112–5120.

(63) Huang, Y.; Ong, C. W.; Yeo, B. S. Effects of Electrolyte Anions on the Reduction of Carbon Dioxide to Ethylene and Ethanol on Copper (100) and (111) Surfaces. *ChemSusChem* **2018**, *11*, 3299–3306.

(64) Yang, Y.; Li, K.; Ajmal, S.; Feng, Y.; Bacha, A.-U.-R.; Nabi, I.; Zhang, L. Interplay between Halides in the Electrolyte and the Chemical States of Cu in Cu-based Electrodes Determines the Selectivity of the C2 Product. *Sus. Energy Fuels* **2020**, *4*, 2284–2292.

(65) Gao, D.; Sinev, I.; Scholten, F.; Arán-Ais, R. M.; Divins, N. J.; Kvashnina, K.; Timoshenko, J.; Roldan Cuenya, B. Selective CO_2 Electroreduction to Ethylene and Multicarbon Alcohols via Electrolyte-Driven Nanostructuring. *Angew. Chem. Inter. Ed.* **2019**, *58*, 17047–17053.

(66) Li, W. H.; Wang, Y.; Ye, J. H.; Li, S. F. Y. In Situ STM Study of Chloride Adsorption on Cu(110) Electrode in Hydrochloric Acid Aqueous Solution. *J. Phys. Chem. B* **2001**, *105*, 1829–1833.

(67) Bae, S.-E.; Gewirth, A. A. In Situ EC-STM Studies of MPS, SPS, and Chloride on Cu(100): Structural Studies of Accelerators for Dual Damascene Electrodeposition. *Langmuir* **2006**, *22*, 10315–10321.

(68) Keller, H.; Saracino, M.; Nguyen, H. M.; Huynh, T. M. T.; Broekmann, P. Competitive Anion/Water and Cation/Water Interactions at Electrified Copper/Electrolyte Interfaces Probed by in Situ X-ray Diffraction. *J. Phys. Chem. C* **2012**, *116*, 11068–11076.

(69) McCrum, I. T.; Akhade, S. A.; Janik, M. J. Electrochemical Specific Adsorption of Halides on Cu 111, 100, and 211: A Density Functional Theory Study. *Electrochim. Acta* **2015**, *173*, 302 – 309.

(70) Weitzner, S. E.; Akhade, S. A.; Varley, J. B.; Wood, B. C.; Otani, M.; Baker, S. E.; Duoss, E. B. Toward Engineering of Solution Microenvironments for the CO_2 Reduction Reaction: Unraveling pH and Voltage Effects from a Combined Density-Functional-Continuum Theory. *J. Phys. Chem. Lett.* **2020**, *11*, 4113–4118.

(71) Varela, A. S.; Ju, W.; Reier, T.; Strasser, P. Tuning the Catalytic Activity

and Selectivity of Cu for CO_2 Electroreduction in the Presence of Halides. *ACS Catal.* **2016**, *6*, 2136–2144.

(72) Ma, W.; Xie, S.; Liu, T.; Fan, Q.; Ye, J.; Sun, F.; Jiang, Z.; Zhang, Q.; Cheng, J.; Wang, Y. A. Electrocatalytic Reduction of CO_2 to Ethylene and Ethanol Through Hydrogen-assisted C-C Coupling over Fluorine-modified Copper. *Nat. Catal.* **2020**, 2520–1158.

Graphical TOC Entry